TWMS J. App. and Eng. Math. V.13, N.2, 2023, pp. 649-660

NUMERICAL SOLUTION OF THE INVERSE GARDNER EQUATION

S. FOADIAN[1], R. POURGHOLI[1*], M. G. BALADEZAEI[2], §

Abstract. In this paper, the numerical solution of the inverse Gardner equation will be considered. The Haar wavelet collocation method (HWCM) will be used to determine the unknown boundary condition which is estimated from an over-specified condition at a boundary. In this regard, we apply the HWCM for discretizing the space derivatives and then use a quasilinearization technique to linearize the nonlinear term in the equations. It is proved that the proposed method has the order of convergence $\mathcal{O}(\Delta x)$. The efficiency and robustness of the proposed approach for solving the inverse Gardner equation are demonstrated by one numerical example.

Keywords: Haar wavelet, Ill-posed inverse problems, Quasilinearization technique, The Tikhonov regularization method.

AMS Subject Classification: 65M32, 65T60.

1. Introduction

Inverse problems have become more and more important in various fields of science and technology. They arise, for example, in the study of heat conduction processes, diffusion, control theory, and have certainly been one of the fastest-growing areas in applied mathematics over the last three decades due partly to its importance in applications. However, as inverse problems typically lead to mathematical models that are ill-posed, their solutions are unstable under data perturbations and classical numerical techniques fail to provide accurate and stable solutions. Fortunately, many methods have been reported to solve the inverse parabolic problems [4, 9, 32, 8] and among the most versatile methods the following can be mentioned: the TR [34, 33], iterative regularization [1], and mollification [24].

Haar wavelets are based on the functions which were introduced by Hungarian mathematician Alfred Haar in 1910. The Haar wavelets are made up of piecewise constant functions and are mathematically the simplest among all the wavelet families. A good

[1] School of Mathematics and Computer Science, Damghan University, Damghan, Iran.
e-mail: s.foadian@std.du.ac.ir; ORCID: https://orcid.org/0000-0001-7091-1254.
e-mail: pourgholi@du.ac.ir; ORCID: https://orcid.org/0000-0003-4111-5130.
[*] Corresponding author.
[2] Department of Applied Mathematics, Islamic Azad University, Damghan Branch, Damghan, Iran.
e-mail: gholami@damghaniau.ac.ir; ORCID: https://orcid.org/0000-0001-9290-7766.
§ Manuscript received: January 11, 2021; accepted: March 05, 2021.

feature of these wavelets is the possibility to integrate them analytically at arbitrary times. They can be interpreted as a first-order Daubechies wavelet. Haar wavelets are the only compactly supported orthogonal wavelets that have explicit formulas. The other wavelets are given implicitly as the recursive procedures [7], and subsequently, they cannot be used directly in identification algorithms when the input signal is random and require designing special computational algorithms ([31, 15]). Due to mathematical simplicity, the Haar wavelet method has turned out to be an effective tool for solving differential and integral equations. Furthermore, the Haar wavelets are very efficient tools for solving the nonlinear systems in physics, biology, chemical reactions, and fluid mechanics [3, 18, 25, 29]. Lepik [20, 19] use Haar wavelets to solve differential and integral equations. Hariharan and Kannan [14, 13] introduced the Haar wavelet method for solving some linear and nonlinear one-dimensional reaction-diffusion equations and the well-known nonlinear parabolic PDEs. In the field of numerical solution of the inverse problems, Pourgholi et al. [28, 27, 26] have used the Haar wavelet method for the solution of a variety of PDEs.

In this paper, as the main problem, we use the HWCM for solving the inverse Gardner equation. The Gardner equation, or the combined KdV and modified-KdV equation, reads [35]

$$u_t + 2\alpha u u_x - 3\beta u^2 u_x + u_{xxx} = 0, \qquad \alpha, \beta > 0, \tag{1}$$

where α and β arbitrary constants, and $u(x,t)$ is the amplitude of the relevant wave mode. Equation (1) is completely integrable, like the KdV equation, by the inverse scattering method. Equation (1) is studied in [35, 10] where new kind of solutions was obtained. The Gardner equation is widely used in various branches of physics, such as plasma physics, fluid physics, quantum field theory, hydrodynamics, and theoretical physics [10, 17, 2, 11, 36, 37]. It also describes a variety of wave phenomena in plasma and solid-state [35, 16]. Various methods for studying integrability properties and exact solutions of the Gardner equation have been reported [35, 22, 23].

We have considered the inverse form of equation (1) in the dimensionless form;

$$u_t + 2\alpha u u_x - 3\beta u^2 u_x + u_{xxx} = 0, \qquad \alpha, \beta > 0, \tag{2}$$

with the initial and boundary conditions

$$u(x,0) = f(x), \qquad x \in \overline{\Omega}_x, \tag{3}$$

$$u(a,t) = g(t), \qquad u(b,t) = q(t), \qquad u_x(b,t) = h(t), \qquad t \in \overline{\Omega}_t, \tag{4}$$

and the overspecified conditions

$$u(\ell,t) = k_1(t), \qquad t \in \overline{\Omega}_t, \tag{5}$$

$$u_x(\ell,t) = k_2(t), \qquad t \in \overline{\Omega}_t, \tag{6}$$

where $\Omega_x = (a,b)$, $\Omega_t = (0,t_F)$, $a < \ell < b$ are fixed points, $f(x)$, $q(t)$, $h(t)$, $k_1(t)$, and $k_2(t)$ are piecewise known continuous functions, and t_F represents the final existence time for the time evolution of the problem, while function $g(t)$ is unknown which remains to be determined from some interior temperature measurements.

The current study aims to clarify the accuracy issues of the HWCM, for solving the inverse Gardner equation (2)–(6), which can be one of the advantages of our method.

The paper is organized as follows: In the next Section, the Haar wavelets family and their integrals are introduced. In the following, Haar matrices for the numerical solutions, the desired issue are described and the expanding functions into the Haar wavelet series are discussed. Also, the convergence analysis of the HWCM is given in this Section. In Section 3, the presented method is detailed for solving the inverse problem (2)–(6). In Section 4, a numerical result is reported and finally, the conclusion is made in Section 5.

2. Haar Wavelets

2.1. **Haar wavelets family and their integrals.** Let us consider the interval $x \in [a, b]$, where a and b are given constants. We define the quantity $M = 2^J$, where J is the maximal level of resolution. The interval $[a, b]$ is divided into $2M$ subintervals of equal length; the length of each subinterval is $\Delta x = \frac{b-a}{2M}$. Next two parameters are introduced; $j = 0, 1, \dots, J$ and $k = 0, 1, \dots, 2^j - 1$. The wavelet number i is identified as $i = 2^j + k + 1$. The i-th Haar wavelet is defined as [21],

$$h_i(x) = \begin{cases} 1, & x \in \big[\xi_1(i), \xi_2(i)\big), \\ -1, & x \in \big[\xi_2(i), \xi_3(i)\big), \\ 0, & \text{elsewhere}, \end{cases} \tag{7}$$

where $\mu = \frac{M}{2^j}$ and

$$\xi_1(i) = a + 2k\mu\Delta x, \qquad \xi_2(i) = a + (2k+1)\mu\Delta x, \qquad \xi_3(i) = a + 2(k+1)\mu\Delta x. \tag{8}$$

These equations are valid if $i > 2$. The case $i = 1$ corresponds to the scaling function:

$$h_1(x) = \begin{cases} 1, & x \in [a, b], \\ 0, & \text{elsewhere}. \end{cases}$$

The parameters j and k have concrete meaning. The support (the width of the i-th wavelet) is

$$\xi_3(i) - \xi_1(i) = 2\mu\Delta x = \frac{b-a}{2^j} = (b-a)2^{-j}.$$

It follows from here that if we increase j then the support decreases (the wavelet becomes more narrow). By this reason it is called the *dilatation parameter*. The other parameter k localises the position of the wavelet in the x-axis; if k changes from 0 to $2^j - 1$ the initial point of the i-th wavelet $\xi_1(i)$ moves from $x = a$ to $x = \frac{a+(2^j-1)b}{2^j}$. The integer k is called the *translation parameter*.

If the maximal level of resolution J is prescribed then it follows from (7) that

$$\int_a^b h_{i_1}(x) h_{i_2}(x)\,\mathrm{d}x = \begin{cases} (b-a)2^{-j}, & i_1 = i_2, \\ 0, & i_1 \neq i_2. \end{cases} \tag{9}$$

So we see that the Haar wavelets are orthogonal to each other. In Section 3, we need the integrals of the Haar functions

$$p_{v,i}(x) = \underbrace{\int_a^x \int_a^x \dots \int_a^x}_{v-\text{times}} h_i(t)\,\mathrm{d}t^v = \frac{1}{(v-1)!} \int_a^x (x-t)^{v-1} h_i(t)\,\mathrm{d}t, \tag{10}$$

where, $v = 1, 2, \dots, n$ and $i = 1, 2, \dots, 2M$. Taking account of (7) these integrals can be calculated analytically; by doing it we obtain

$$p_{v,i}(x) = \begin{cases} 0, & x < \xi_1(i), \\ \frac{1}{v!}[x - \xi_1(i)]^v, & x \in [\xi_1(i), \xi_2(i)], \\ \frac{1}{v!}\Big\{[x - \xi_1(i)]^v - 2[x - \xi_2(i)]^v\Big\}, & x \in [\xi_2(i), \xi_3(i)], \\ \frac{1}{v!}\Big\{[x - \xi_1(i)]^v - 2[x - \xi_2(i)]^v + [x - \xi_3(i)]^v\Big\}, & x > \xi_3(i). \end{cases} \tag{11}$$

These formulas hold for $i > 1$. In the case $i = 1$ we have $\xi_1(1) = a$, $\xi_2(1) = \xi_3(1) = b$ and

$$p_{v,1}(x) = \frac{1}{v!}(x-a)^v. \tag{12}$$

2.2. **Haar matrices.** If we want to use the Haar wavelets for the numerical solutions we must put them into a discrete form. There are different ways to do it; in this paper, the collocation method is applied. The collocation points defined as

$$x_l = a + (l - 0.5)\Delta x, \qquad l = 1, 2, \dots, 2M, \tag{13}$$

and replace $x \to x_l$ in equations (7), (11), and (12). It is convenient to put these results into the matrix form. For this, we introduce the Haar matrices H, P_1, P_2, $\dots$, P_v which are $2M \times 2M$ matrices. The elements of these matrices are $H(i,l) = h_i(x_l)$ and $P_v(i,l) = p_{v,i}(x_l)$, $v = 1, 2, \dots, n$.

2.3. **Expanding functions into the Haar wavelet series.** This Section aims to describe a new modification of the Haar wavelet method for solving the inverse Gardner equation (2). It is known that any integrable function $u(x) \in \mathcal{L}^2([a,b])$ can be expanded by a Haar series with an infinite number of terms [28],

$$u(x) = \sum_{i=1}^{\infty} c_i h_i(x),$$

where the Haar wavelet coefficients are determined as

$$c_i = \frac{2^j}{b-a} \int_a^b u(x) h_i(x)\,\mathrm{d}x, \qquad i = 2^j + k + 1, \quad j \geq 0,\ 0 \leq k < 2^j,$$

specially $c_1 = \frac{1}{b-a}\int_a^b u(x)\,\mathrm{d}x$. So, $u(x) = c_1 h_1(x) + \sum_{j=0}^{\infty}\sum_{k=0}^{2^j-1} c_{2^j+k+1} h_{2^j+k+1}(x)$. If $u(x)$ is piecewise constant by itself, or may be approximated as piecewise constant during each subinterval, then $u(x)$ will be terminated at finite terms, that is

$$u_J(x) \cong c_1 h_1(x) + \sum_{j=0}^{J}\sum_{k=0}^{2^j-1} c_{2^j+k+1} h_{2^j+k+1}(x) = C_{2M}^T H_{2M}(x), \tag{14}$$

where the coefficient C_{2M}^T and the Haar function vectors $H_{2M}(x)$ are defined as

$$C_{2M}^T = \Big(c_1, c_2, \dots, c_{2M}\Big), \qquad H_{2M}(x) = \Big(h_1(x), h_2(x), \dots, h_{2M}(x)\Big)^T,$$

2.4. **Convergence analysis of the Haar wavelet method.** In this Section, we present the error analysis for our proposed scheme. In order to analyze the convergence of our method, we assume that $u_J(x)$ is approximation solution of $u(x)$. The corresponding error at J-th level of $u(x)$ is defined as

$$e_J(x) = u(x) - u_J(x) = \sum_{j=J+1}^{\infty}\sum_{k=0}^{2^j-1} c_{2^j+k+1} h_{2^j+k+1}(x).$$

Now, we state and prove the following convergence theorem:

Theorem 2.1. *Suppose that $u(x)$ satisfy the Lipschitz condition on $[a,b]$, that is,*

$$\exists\ \kappa > 0,\ \forall\ x_1, x_2 \in [a,b]\ :\ |u(x_1) - u(x_2)| \leq \kappa |x_1 - x_2|. \tag{15}$$

Then the error bound for $\|e_J\|_2$ is obtained as $\|e_J\|_2 \leq \frac{\kappa(b-a)}{\sqrt{6}}\Delta x$. Also, the HWCM will converge in the sense that $e_J(x)$ go to zero as M goes to infinity. Moreover, the convergence is of order one, that is, $\|e_J\|_2 = \mathcal{O}(\Delta x)$.

Proof. We compute $\|e_J\|_2^2$ as the following:

$$\|e_J\|_2^2 = \int_a^b \Big(\sum_{j=J+1}^{\infty} \sum_{k=0}^{2^j-1} c_{2^j+k+1} h_{2^j+k+1}(x) \Big)^2 \,\mathrm{d}x$$
$$= \sum_{j=J+1}^{\infty} \sum_{k=0}^{2^j-1} \sum_{l=J+1}^{\infty} \sum_{q=0}^{2^l-1} c_{2^j+k+1} c_{2^l+q+1} \left(\int_a^b h_{2^j+k+1}(x) h_{2^l+q+1}(x) \,\mathrm{d}x \right).$$

Taking account of (9), we have

$$\|e_J\|_2^2 = \sum_{j=J+1}^{\infty} \sum_{k=0}^{2^j-1} \frac{b-a}{2^j}\, c^2_{2^j+k+1}$$

and since, $c_{2^j+k+1} = \frac{2^j}{b-a} \int_a^b u(x) h_{2^j+k+1}(x)\,\mathrm{d}x$, according to the Haar wavelet functions (7), we can write

$$c_{2^j+k+1} = \frac{2^j}{b-a} \left(\int_{\xi_1(2^j+k+1)}^{\xi_2(2^j+k+1)} u(x)\,\mathrm{d}x - \int_{\xi_2(2^j+k+1)}^{\xi_3(2^j+k+1)} u(x)\,\mathrm{d}x \right).$$

Now, using the mean value theorem for integral, we can conclude

$$\exists\ x_1 \in \Big[\xi_1(2^j+k+1), \xi_2(2^j+k+1)\Big],\ x_2 \in \Big[\xi_2(2^j+k+1), \xi_3(2^j+k+1)\Big],$$

such that

$$\int_{\xi_1(2^j+k+1)}^{\xi_2(2^j+k+1)} u(x)\,\mathrm{d}x = \frac{b-a}{2^{j+1}} u(x_1), \qquad \int_{\xi_2(2^j+k+1)}^{\xi_3(2^j+k+1)} u(x)\,\mathrm{d}x = \frac{b-a}{2^{j+1}} u(x_2).$$

Thus, we can compute c_{2^j+k+1} as follows;

$$c_{2^j+k+1} = \frac{2^j}{b-a} \left(\frac{b-a}{2^{j+1}} u(x_1) - \frac{b-a}{2^{j+1}} u(x_2) \right) = \frac{1}{2}\Big(u(x_1) - u(x_2)\Big) \leq \frac{1}{2}\kappa\Big(x_1 - x_2\Big) \leq \frac{b-a}{2^{j+1}}\,\kappa.$$

The first inequality is obtained with regard to relation (15). On the other hand, we have

$$\|e_J^u\|_2^2 = \sum_{j=J+1}^{\infty} \sum_{k=0}^{2^j-1} \frac{b-a}{2^j}\, c^2_{2^j+k+1} \leq \sum_{j=J+1}^{\infty} \sum_{k=0}^{2^j-1} \frac{b-a}{2^j}\, \kappa^2\, \frac{(b-a)^2}{2^{2j+2}} = \frac{(b-a)^3}{3} \kappa^2 \Big(\frac{1}{4}\Big)^{J+1}.$$

Since $2M = 2^{J+1}$, we obtain

$$\|e_J\|_2^2 \leq \frac{(b-a)^3}{3} \kappa^2 \Big(\frac{1}{2M}\Big)^2.$$

Therefore, the error bound can be expressed as

$$\|e_J\|_2 \leq \frac{\kappa(b-a)}{\sqrt{3}} \Delta x.$$

So, the Haar wavelet method will be convergent, i.e., $\lim_{J\to\infty} e_J(x) = 0$. Moreover, the convergence is of order one, that is, $\|e_J\|_2 = \mathcal{O}(\Delta x)$, and the proof is complete. □

3. Solution Of The Inverse Gardner Equation

In this section, we first present our method based on the HWCM for solving the inverse Gardner equation (2)–(6). Then, to get to an ill-posed system, we introduce the TR method to obtain a stable approximation of the solution of the final system.

Let us divide the interval $[0, t_F]$ into N equal parts of length $\Delta t = \frac{t_F}{N}$ and denote $t_s = (s-1)\Delta t,\ s = 1, 2, \ldots, N$. We assume that $\dot{u}'''(x,t)$, can be expanded in terms of the Haar wavelets as, [6],

$$\dot{u}'''(x,t) \cong c_1^s h_1(x) + \sum_{j=0}^{J} \sum_{k=0}^{2^j-1} c^s_{2^j+k+1} h_{2^j+k+1}(x) = C^T_{2M} H_{2M}(x), \tag{16}$$

where dot and prime mean differentiation with respect to t and x, respectively. Also, the vector C^T_{2M} is constant in each subinterval $[t_s, t_{s+1}],\ s = 1, 2, \ldots, N$.

We integrate (16) one time with respect to t from t_s to t and three times with respect to x from ℓ to x. These, respectively, yield

$$u'''(x,t) = (t - t_s) C^T_{2M} H_{2M}(x) + u'''(x, t_s), \tag{17}$$

$$\dot{u}'(x,t) = C^T_{2M} P_2(x) + \dot{u}'(\ell, t) + (x - \ell)\dot{u}''(\ell, t), \tag{18}$$

$$\dot{u}(x,t) = C^T_{2M} P_3(x) + \dot{u}(\ell, t) + (x - \ell)\dot{u}'(\ell, t) + \frac{(x-\ell)^2}{2}\dot{u}''(\ell, t), \tag{19}$$

where, $P_2(x) = p_{2,i}(x)$ and $P_3(x) = p_{3,i}(x)$ are obtained from (10). Now, integrating formula (18), with respect to t from t_s to t, we obtain

$$u'(x,t) = (t-t_s)C^T_{2M} P_2(x) + u'(x, t_s) + u'(\ell, t) - u'(\ell, t_s) + (x-\ell)[u''(\ell, t) - u''(\ell, t_s)]. \tag{20}$$

By using the boundary conditions $u(b,t)$ and $u_x(b,t)$ and overspecified conditions (5) and (6), equations (19) and (20) are changed as follows:

$$\begin{aligned} \dot{u}(x,t) = C^T_{2M}\Big[P_3(x) - \frac{(x-\ell)^2}{(b-\ell)^2} P_3(b)\Big] + \Big[1 - \frac{(x-\ell)^2}{(b-\ell)^2}\Big] k_1'(t) \\ + \Big[(x-\ell) - \frac{(x-\ell)^2}{b-\ell}\Big] k_2'(t) + \frac{(x-\ell)^2}{(b-\ell)^2} q'(t), \end{aligned} \tag{21}$$

$$\begin{aligned} u'(x,t) = (t - t_s) C^T_{2M}\Big[P_2(x) - \frac{x-\ell}{b-\ell} P_2(b)\Big] + u'(x, t_s) \\ + \frac{x-\ell}{b-\ell}\Big[h(t) - h(t_s)\Big] + \Big[1 - \frac{x-\ell}{b-\ell}\Big]\Big[k_2(t) - k_2(t_s)\Big]. \end{aligned} \tag{22}$$

Now, individual integrating of equation (21) with respect to t, yield

$$\begin{aligned} u(x,t) =& (t - t_s) C^T_{2M}\Big[P_3(x) - \frac{(x-\ell)^2}{(b-\ell)^2} P_3(b)\Big] + \Big[1 - \frac{(x-\ell)^2}{(b-\ell)^2}\Big]\Big[k_1(t) - k_1(t_s)\Big] \\ &+ \Big[(x-\ell) - \frac{(x-\ell)^2}{b-\ell}\Big]\Big[k_2(t) - k_2(t_s)\Big] + \frac{(x-\ell)^2}{(b-\ell)^2}\Big[q(t) - q(t_s)\Big] + u(x, t_s). \end{aligned} \tag{23}$$

Discretizing the results (17) and (21)–(23), by assuming $x \to x_l$, $t \to t_{s+1}$ and using notation $\Delta t = t_{s+1} - t_s$ we obtain

$$u'''(x_l, t_{s+1}) = \Delta t C_{2M}^T H_{2M}(x_l) + u'''(x_l, t_s), \tag{24}$$

$$\dot{u}(x_l, t_{s+1}) = C_{2M}^T\Big[P_3(x_l) - \frac{(x_l-\ell)^2}{(b-\ell)^2}P_3(b)\Big] + \Big[1 - \frac{(x_l-\ell)^2}{(b-\ell)^2}\Big]k_1'(t_{s+1}) - (x_l-\ell)\frac{x_l-b}{b-\ell}k_2'(t_{s+1}) + \frac{(x_l-\ell)^2}{(b-\ell)^2}q'(t_{s+1}), \tag{25}$$

$$u'(x_l, t_{s+1}) = \Delta t C_{2M}^T\Big[P_2(x_l) - \frac{x_l-\ell}{b-\ell}P_2(b)\Big] + u'(x_l, t_s) + \frac{x_l-\ell}{b-\ell}\Big[h(t_{s+1}) - h(t_s)\Big] - \frac{x_l-b}{b-\ell}\Big[k_2(t_{s+1}) - k_2(t_s)\Big], \tag{26}$$

$$u(x_l, t_{s+1}) = \Delta t C_{2M}^T\Big[P_3(x_l) - \frac{(x_l-\ell)^2}{(b-\ell)^2}P_3(b)\Big] + \Big[1 - \frac{(x_l-\ell)^2}{(b-\ell)^2}\Big]\Big[k_1(t_{s+1}) - k_1(t_s)\Big] + u(x_l, t_s) - (x_l-\ell)\frac{x_l-b}{b-\ell}\Big[k_2(t_{s+1}) - k_2(t_s)\Big] + \frac{(x_l-\ell)^2}{(b-\ell)^2}\Big[q(t_{s+1}) - q(t_s)\Big]. \tag{27}$$

Here, the well known technique quasilinearization is used to tackle the nonlinearity terms in equation (2) ([5]). So, we have

$$u(x,t)u_x(x,t) = u_x(x,t_s)u(x,t_{s+1}) + u(x,t_s)u_x(x,t_{s+1}) - u(x,t_s)u_x(x,t_s),$$
$$u^2(x,t)u_x(x,t) = 2u(x,t_s)u_x(x,t_s)u(x,t_{s+1}) - 2(u(x,t_s))^2u_x(x,t_s) + u^2(x,t_s)u_x(x,t_{s+1}).$$

Therefore, the nonlinear equation (2) is as follows:

$$\dot{u}(x,t_{s+1}) + \Big[2\alpha u_x(x,t_s) - 6\beta u(x,t_s)u_x(x,t_s)\Big]u(x,t_{s+1}) + u'''(x,t_{s+1}) + \Big[2\alpha u(x,t_s) - 3\beta u^2(x,t_s)\Big]u_x(x,t_{s+1}) = 2\alpha u(x,t_s)u_x(x,t_s) - 6\beta u^2(x,t_s)u_x(x,t_s). \tag{28}$$

Now, discretizing the result (28) by $x \to x_l$ and using equations (24)–(27), we have

$$C_{2M}^T\Bigg[(1+\mathcal{R}_1\Delta t)\Big[P_3(x_l) - \frac{(x_l-\ell)^2}{(b-\ell)^2}P_3(b)\Big] + \mathcal{R}_2\Delta t\Big[P_2(x_l) - \frac{x_l-\ell}{b-\ell}P_2(b)\Big] + \Delta t H_{2M}(x_l)\Bigg] = 2\alpha u(x_l,t_s)u_x(x_l,t_s) - 6\beta u^2(x_l,t_s)u_x(x_l,t_s) - u'''(x_l,t_s)$$
$$- \Bigg[\Big[1 - \frac{(x_l-\ell)^2}{(b-\ell)^2}\Big]k_1'(t_{s+1}) - (x_l-\ell)\frac{x_l-b}{b-\ell}k_2'(t_{s+1}) + \frac{(x_l-\ell)^2}{(b-\ell)^2}q'(t_{s+1})\Bigg]$$
$$- \mathcal{R}_1\Bigg[\Big[1 - \frac{(x_l-\ell)^2}{(b-\ell)^2}\Big]\Big[k_1(t_{s+1}) - k_1(t_s)\Big] - (x_l-\ell)\frac{x_l-b}{b-\ell}\Big[k_2(t_{s+1}) - k_2(t_s)\Big] + \frac{(x_l-\ell)^2}{(b-\ell)^2}\Big[q(t_{s+1}) - q(t_s)\Big] + u(x_l,t_s)\Bigg]$$
$$- \mathcal{R}_2\Bigg[u'(x_l,t_s) + \frac{x_l-\ell}{b-\ell}\Big[h(t_{s+1}) - h(t_s)\Big] - \frac{x_l-b}{b-\ell}\Big[k_2(t_{s+1}) - k_2(t_s)\Big]\Bigg], \tag{29}$$

where

$$\mathcal{R}_1 = 2\alpha u_x(x_l,t_s) - 6\beta u(x_l,t_s)u_x(x_l,t_s), \qquad \mathcal{R}_2 = 2\alpha u(x_l,t_s) - 3\beta u^2(x_l,t_s).$$

From the equation (29), a system of $2M$ linear equations in the $2M$ unknown coefficients is obtained. This system can be written in the matrix vector form as follows:

$$\mathcal{A}\mathcal{X} = \mathcal{B}. \tag{30}$$

The solution of the linear algebraic equation (30) for vector $\mathcal{X}$ can be get by the TR method ([34, 12]).

4. Numerical Experiments

In this section, we apply the HWCM as discussed in Section 3, to obtain the numerical solution for unknown boundary condition in the problem (2)–(6). The proposed method is written in the MATLAB 7.14 (R2012a) and is tested on a personal computer with Intel(R) Core(TM)2 Duo CPU and 4GB RAM.

To illustrate the performance of the method and justify the accuracy and efficiency of the proposed method, we considered one test example. To this end, we take $a = 0$, $b = 1$, $\alpha = \beta = 1$, $\ell = 0.5$, $t_F = 1$, $\Delta t = 0.01$, and the noisy data=input data+0.001×rand$n$. Numerical results are compared with the Legendre wavelet method [30].

Remark 4.1. *The error norm L_∞ and the root mean square (RMS) error norm, are calculated to measure the accuracy of the numerical scheme using following formulas:*

$$L_\infty = ||u(x,t) - u^*(x,t)||_\infty = \max_{1\leq i\leq 2M} |u(x_i,t) - u^*(x_i,t)|,$$

$$RMS = \left[\frac{1}{2M}\sum_{i=1}^{2M}\Big(u(x_i,t) - u^*(x_i,t)\Big)^2\right]^{\frac{1}{2}},$$

where, $u^*(x,t)$ is the estimated value of $u(x,t)$.

Example 4.1. *We consider the inverse Gardner equation* (2)–(6) *satisfying,*

$$u_t + 2uu_x - 3u^2u_x + u_{xxx} = 0, \qquad x \in \Omega_x, \quad t \in \Omega_t.$$

The exact solution of this problem is, ([35]*),*

$$u(x,t) = \frac{1}{3}\left[1 - \tanh\Big(\frac{1}{3\sqrt{2}}(x - \frac{2}{9}t)\Big)\right], \qquad x \in \overline{\Omega}_x, \quad t \in \overline{\Omega}_t,$$

$$u(0,t) = \frac{1}{3}\left[1 + \tanh\Big(\frac{\sqrt{2}}{27}t\Big)\right], \qquad t \in \overline{\Omega}_t.$$

The numerical results of the unknown boundary condition $u(0,t) = g(t)$ are reported in Table 1. Furthermore, Table 2 reports the absolute error (L_∞) and RMS error $u(x,t)$, for different time steps. Figures 1–3, show the physical behavior of numerical solutions, in 2-dimensional, 3-dimensional, and contour forms when $J = 1$ and $J = 4$, respectively.

5. Conclusions

In this paper, we applied the HWCM to estimate unknown boundary condition for the inverse Gardner equation (2)–(6). The convergence rate of the proposed method has been discussed and shown that it is $\mathcal{O}(\Delta x)$. Numerical comparisons have been made between the implementations of the proposed method and the Legendre wavelet method. Due to the numerical solutions which are presented in the Tables and Figures, the obtained numerical solutions by the presented method are the most accurate in comparison with the Legendre wavelet method and are in good agreement with the exact solutions. The

TABLE 1. The comparison among the exact and numerical solutions for $g(t)$.

		Haar wavelet ($2M = 4$)		Legendre wavelet ($k = 1$, $M = 4$)	
t	$g(t)$	$g^*(t)$	$\|g(t) - g^*(t)\|$	$g^*(t)$	$\|g(t) - g^*(t)\|$
0.1	0.335079	0.335079	$5.821170e-07$	0.335068	$1.131338e-05$
0.2	0.336825	0.336824	$1.171149e-06$	0.336905	$8.018074e-05$
0.3	0.338571	0.338569	$1.767145e-06$	0.338654	$8.283780e-05$
0.4	0.340316	0.340314	$2.369855e-06$	0.340438	$1.221634e-04$
0.5	0.342061	0.342058	$2.979024e-06$	0.342239	$1.777258e-04$
0.6	0.343806	0.343802	$3.594395e-06$	0.344011	$2.050502e-04$
0.7	0.345549	0.345545	$4.215701e-06$	0.345803	$2.539438e-04$
0.8	0.347293	0.347288	$4.842675e-06$	0.347561	$2.686224e-04$
0.9	0.349035	0.349030	$5.475044e-06$	0.349348	$3.123698e-04$
1	0.350777	0.350771	$6.112529e-06$	0.351077	$2.997438e-04$
CPU time (s)		0.944683		86.357375	

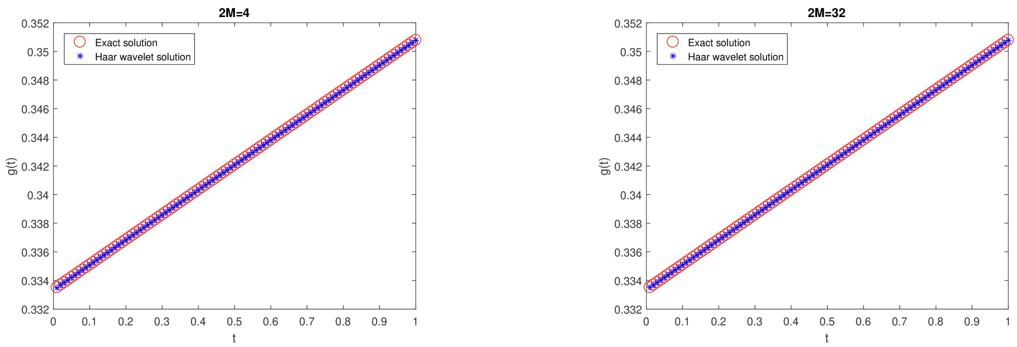

FIGURE 1. Comparison between the exact and numerical solutions $g(t)$ in 2-dimensional graph using the HWCM.

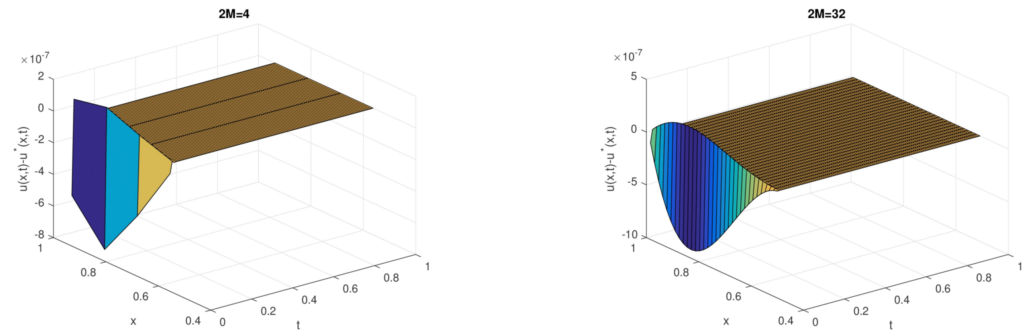

FIGURE 2. Comparison between the exact and numerical solutions $u(x,t)$ in 3-dimensional graph using the HWCM.

strong point of this method is its easy and simple computation with low-storage space and cost.

TABLE 2. The absolute error (L_∞) and RMS error $u(x,t)$, for different values of t.

t	Haar wavelet ($2M=4$)		Legendre wavelet ($k=1$, $M=4$)	
	L_∞	RMS	L_∞	RMS
0.1	$4.364209e-11$	$2.797793e-11$	$2.218248e-05$	$1.118012e-05$
0.3	$1.291322e-10$	$9.569208e-11$	$7.173131e-05$	$4.407432e-05$
0.5	$2.172547e-10$	$1.597837e-10$	$1.172653e-04$	$7.840790e-05$
0.7	$3.079276e-10$	$2.192898e-10$	$1.573861e-04$	$1.077401e-04$
1	$4.483989e-10$	$3.008370e-10$	$2.049956e-04$	$1.353533e-04$
CPU time (s)	0.944683		86.357375	
t	Haar wavelet ($2M=8$)		Legendre wavelet ($k=1$, $M=8$)	
	L_∞	RMS	L_∞	RMS
0.1	$3.073597e-12$	$1.960665e-12$	$7.381023e-05$	$2.979840e-05$
0.3	$4.176554e-11$	$2.595888e-11$	$8.894824e-05$	$3.956907e-05$
0.5	$8.116213e-11$	$5.070258e-11$	$1.526883e-04$	$8.417704e-05$
0.7	$1.178229e-10$	$7.365077e-11$	$2.071996e-04$	$1.158957e-04$
1	$1.674241e-10$	$1.045204e-10$	$2.732977e-04$	$1.401590e-04$
CPU time (s)	2.376038		163.189158	
t	Haar wavelet ($2M=16$)		Legendre wavelet ($k=1$, $M=16$)	
	L_∞	RMS	L_∞	RMS
0.1	$1.489231e-11$	$9.849202e-12$	$3.331613e-05$	$9.516170e-06$
0.3	$5.648260e-12$	$3.837684e-12$	$1.141762e-04$	$5.397525e-05$
0.5	$4.939937e-12$	$3.048181e-12$	$2.122533e-04$	$9.720945e-05$
0.7	$1.470157e-11$	$9.397067e-12$	$2.430660e-04$	$1.190776e-04$
1	$2.814687e-11$	$1.812136e-11$	$3.399978e-04$	$1.653103e-04$
CPU time (s)	7.071569		324.216722	
t	Haar wavelet ($2M=32$)		Legendre wavelet ($k=1$, $M=32$)	
	L_∞	RMS	L_∞	RMS
0.1	$2.190170e-11$	$1.434979e-11$	$3.905646e-05$	$1.380812e-05$
0.3	$1.895811e-11$	$1.243817e-11$	$1.207854e-04$	$3.850523e-05$
0.5	$1.668449e-11$	$1.095391e-11$	$1.953040e-04$	$7.795909e-05$
0.7	$1.454431e-11$	$9.558472e-12$	$2.614209e-04$	$1.076496e-04$
1	$1.159794e-11$	$7.641397e-12$	$3.461528e-04$	$1.467908e-04$
CPU time (s)	24.244557		674.541283	

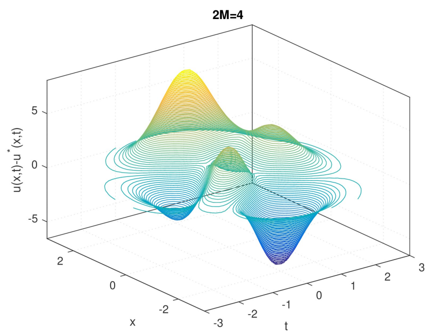

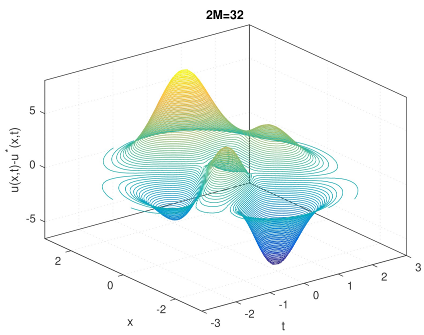

FIGURE 3. Comparison between the exact and numerical solutions $u(x,t)$ in contour plot using the HWCM.

References

[1] Alifanov, O. M., (2012). Inverse heat transfer problems, Springer Science & Business Media.

[2] Antonova, M., Biswas, A., (2009). Adiabatic parameter dynamics of perturbed solitary waves, Communications in Nonlinear Science and Numerical Simulation, 14 (3), pp. 734-748.

[3] Aziz, I., Khan, F., (2014). A new method based on Haar wavelet for the numerical solution of two-dimensional nonlinear integral equations, Journal of Computational and Applied Mathematics, 272, pp. 70-80.

[4] Beck, J. V., Blackwell, B., St Clair Jr, C. R., (1985). Inverse Heat Conduction: Ill-Posed Problems, A Wiley-Interscience, New York.

[5] Bellman, R. E., Kalaba, R. E., (1965). Quasilinearization and nonlinear boundary-value problems, Rand Corporation.

[6] Chen, C. F., Hsiao, C. H., (1997). Haar wavelet method for solving lumped and distributed-parameter systems, IEE Proceedings-Control Theory and Applications, 144 (1), pp. 87-94.

[7] Daubechies, I., Sweldens, W., (1998). Factoring wavelet transforms into lifting steps, Journal of Fourier analysis and applications, 4 (3), pp. 247-269.

[8] Foadian, S., Pourgholi, R., Tabasi, S. H., (2018). Cubic B-spline method for the solution of an inverse parabolic system, Applicable Analysis, 97 (3), pp. 438-465.

[9] Foadian, S., Pourgholi, R., Tabasi, S. H., Damirchi, J., (2019). The inverse solution of the coupled nonlinear reaction–diffusion equations by the Haar wavelets, International Journal of Computer Mathematics, 96 (1), pp. 105-125.

[10] Fu, Z. Liu, S., Liu, S., (2004). New kinds of solutions to Gardner equation, Chaos, Solitons & Fractals, 20 (2), pp. 301-309.

[11] Girgis, L., Biswas, A., (2011). A study of solitary waves by He's semi-inverse variational principle, Waves in Random and Complex Media, 21 (1), pp. 96-104.

[12] Hansen, P. C., (1992). Analysis of discrete ill-posed problems by means of the L-curve, SIAM review, 34 (4), 561-580.

[13] Hariharan, G., Kannan, K., (2010). Haar wavelet method for solving some nonlinear parabolic equations, Journal of mathematical chemistry, 48 (4), pp. 1044-1061.

[14] Hariharan, G., Kannan, K., (2011). A comparative study of Haar wavelet method and homotopy perturbation method for solving one-dimensional reaction-diffusion equations, International Journal of Applied Mathematics and Computation, 3 (1), pp. 21-34.

[15] Härdle, W., Kerkyacharian, G., Picard, D., Tsybakov, A., (2012). Wavelets, approximation, and statistical applications, Springer Science & Business Media, 129.

[16] Konno, K., Ichikawa, Y., (1974). A modified Korteweg de Vries equation for ion acoustic waves, Journal of the Physical Society of Japan, 37 (6), pp. 1631-1636.

[17] Krishnan, E. V., Triki, H., Labidi, M., Biswas, A., (2011). A study of shallow water waves with Gardner's equation, Nonlinear Dynamics, 66 (4), pp. 497-507.

[18] Kumar, M., Pandit, S., (2014). A composite numerical scheme for the numerical simulation of coupled Burgers' equation, Computer Physics Communications, 185 (3), pp. 809-817.

[19] Lepik, Ü., (2008). Solving integral and differential equations by the aid of non-uniform Haar wavelets, Applied Mathematics and Computation, 198 (1), pp. 326-332.

[20] Lepik, Ü., (2009). Haar wavelet method for solving stiff differential equations, Mathematical Modelling and Analysis, 14 (4), pp. 467-481.

[21] Lepik, Ü., Hein, H., (2014). Haar wavelets: with applications, Springer Science & Business Media.

[22] Malfliet, W., Hereman, W., (1996). The tanh method: I. Exact solutions of nonlinear evolution and wave equations, Physica Scripta, 54 (6), pp. 563.

[23] Mohamad, M. N. B., (1992). Exact solutions to the combined KdV and MKdV equation, Mathematical methods in the applied sciences, 15 (2), pp. 73-78.

[24] Murio, D. A., (2011). The mollification method and the numerical solution of ill-posed problems, John Wiley & Sons.

[25] Patra, A., Ray, S. S., (2014). Two-dimensional Haar wavelet Collocation Method for the solution of Stationary Neutron Transport Equation in a homogeneous isotropic medium, Annals of Nuclear Energy, 70, pp. 30-35.

[26] Pourgholi, R., Esfahani, A., Foadian, S., Parehkar, S., (2013). Resolution of an inverse Problem by Haar basis and Legendre wavelet methods, International Journal of Wavelets, Multiresolution and Information Processing, 11 (05), pp. 1350034.

[27] Pourgholi, R., Foadian, S., Esfahani, A., (2013). Haar basis method to solve some inverse problems for two-dimensional parabolic and hyperbolic equations, TWMS Journal of Applied and Engineering Mathematics, 3 (1), pp. 10-32.

[28] Pourgholi, R., Tavallaie, N., Foadian, S., (2012). Applications of Haar basis method for solving some ill-posed inverse problems, Journal of Mathematical Chemistry, 50 (8), pp. 2317-2337.

[29] Ray, S. S., Gupta, A. K., (2014). Comparative analysis of variational iteration method and Haar wavelet method for the numerical solutions of Burgers–Huxley and Huxley equations, Journal of mathematical chemistry, 52 (4), pp. 1066-1080.

[30] Shen, L., Zhu, S., Liu, B., Zhang, Z., Cui, Y., (2020). Numerical implementation of nonlinear system of fractional Volterra integral–differential equations by Legendre wavelet method and error estimation, Numerical Methods for Partial Differential Equations.

[31] Sliwinski, P., Hasiewicz, Z., (2008). Computational algorithms for wavelet identification of nonlinearities in Hammerstein systems with random inputs, IEEE Transactions on Signal Processing, 56 (2), pp. 846-851.

[32] Tadi, M., (1997). Inverse heat conduction based on boundary measurement, Inverse Problems, 13 (6), pp. 1585.

[33] Tikhonov, V. Y., Arsenin, A. N., (1977). Solutions of ill-posed problems, Washington, DC: VH Winston & Sons.

[34] Tikhonov, A. N., Goncharsky, A. V., Stepanov, V. V., Yagola, A. G., (2013). Numerical methods for the solution of ill-posed problems, Springer Science & Business Media, 328.

[35] Wazwaz, A. M., (2007). New solitons and kink solutions for the Gardner equation, Communications in nonlinear science and numerical simulation, 12 (8), pp. 1395-1404.

[36] Xu, G. Q., Li, Z. B., Liu, Y. P., (2003). Exact solutions to a large class of nonlinear evolution equations, Chinese Journal of Physics, 41 (3), pp. 232-241.

[37] Yan, Z., (2003). Jacobi elliptic function solutions of nonlinear wave equations via the new sinh-Gordon equation expansion method, Journal of Physics A: Mathematical and General, 36 (7), pp. 1961.

Saedeh Foadian received her B.Sc. degree in applied mathematics (2009), M.Sc. degree in harmonic analysis (2012), and Ph.D. degree in 2018 in Applied Mathematics Damghan University, Iran. Her area of research is the numerical solution of the inverse linear and nonlinear parabolic problems.

Reza Pourgholi for the photography and short autobiography, see TWMS J. App. and Eng. Math. V.13, N.2.

Mohammad Gholami Baladezaei received his B.Sc. degree in 1997 from Tabriz University and M.Sc. degree in 2000 from K. N. Toosi University of Technology in applied mathematics. He is currently a PHD student in Applied Mathematics at Fredowsi University of Mashhad, Iran. His area of research is the numerical analysis and optimal control problems and financial mathematics.